



Using a Photochemical Index to Discuss the Ozone Formation and Estimate Hydroxyl Concentration at Downwind Area

Kuo-Hsin Tseng¹, Jia-Lin Wang², Pei-Hsuan Kuo¹, Ben-Jei Tsuang^{1*}

¹ Department of Environmental Engineering, National Chung-Hsing University, Taichung, 402, Taiwan

² Department of Chemistry, National Central University, Taoyuan, 320, Taiwan

ABSTRACT

Ozone problem is deteriorating in the mountainous areas in central Taiwan. High level of reactive ozone precursor coming from traffic, industrial activities and vegetation upwind produces ozone episodes in the downwind area. Continuously monitoring of ozone and its precursors with hourly resolution was performed by three photochemical assessment monitoring stations (PAMS) forming a line of upwind, midway and downwind observation. A ratio (ethylbenzene/m, p-xylene) which showed high agreement with ozone concentrations were used as a sensitive photochemical index to represent the degree of photochemical reaction. It was found that both the peaks of the photochemical index and the ozone concentration around noon exhibited a consistent descending order of Jhushan (downwind) > Caotun (midway) > Chonglun (upwind). Furthermore, when coupling photochemical index of the three PAMS with kinetic equations and the trajectory model, OH concentrations were estimated. The results showed that the OH concentration reached the maximum (2.1×10^6 - 2.3×10^6 molecule/cm³) at noon to early afternoon on a daily cycle.

Keywords: Volatile organic compounds; Photochemical index; Backward trajectory; OH concentration.

INTRODUCTION

Owing to the rapid population growth and economic development, large amount of air pollutants were released into the atmosphere at an unprecedented rate in recent decades. However, the instate of effective control policies and application of pollutant control equipment, the concentrations of key air pollutants, including particulate matter (PM₁₀), carbon monoxide (CO), sulfur dioxide (SO₂) and nitrogen dioxide (NO₂), showed a decreasing trend in the last decades, with SO₂ being the more successfully controlled species. Secondary aerosol and ozone are major air pollution issues in Taiwan (Hsieh *et al.*, 2009). Surprisingly, the trend of ozone (O₃) concentration and the number of O₃ episode days gradually increased during the same time period (Fig. 1). Note that the day which hourly maximum of O₃ concentration in 24 hours exceeds 96 ppb is defined as O₃ episode. O₃ is an oxidant with high reactivity and was proved to have adverse effect on human health and plants (Beckett, 1991; Fuhrer *et al.*, 1997; Leeuw *et al.*, 2000). Moreover, O₃ is a greenhouse gas by absorbing infrared, thus contributing to climate change (Last, 1993; Wilson *et al.*, 2007; Judith *et al.*, 2008; Son *et al.*, 2008).

The O₃ is a secondary pollutant produced by a series of photochemical reactions of nitrogen oxides (NO_x) and volatile organic compounds (VOCs) (Leeuw *et al.*, 2000; De Leeuw, 2002; Derwent *et al.*, 2007; Kumar *et al.*, 2008; Martins and Andrade, 2008; Yang *et al.*, 2008). The relation between reactants and products can be analyzed through observed of VOCs, NO_x and O₃ (Kassomenos *et al.*, 1999; De Leeuw, 2000). In Taiwan, O₃ and its precursors have been systematically monitored by the networks of air quality monitoring station (AQMS) and PAMS

respectively, for more than a decade. They also provide accurate representative information which can be used as an important basis for genetic analysis or control strategy. According to the station location related pollutant transmission trajectory, PAMS can be categorized into four types: Type 1 is the windward station with the background characteristic for an interesting area. Type 2 is the station with the highest concentration of O₃ precursors. Type 3 is the station with the highest concentration of O₃ and Type 4 is the station with farthest downwind.

Reactivity of VOCs on O₃ formation is highly compound dependent and numerous VOCs can be found in the atmosphere, including alkanes, alkenes, aromatic compounds, aldehydes, ketones and polycyclic aromatic hydrocarbons (PAHs), etc. (Cater *et al.*, 1994; Martins and Andrade, 2008). In the actual atmospheric environment, VOCs react with hydroxyl radicals (OH) involving complex reactions forming O₃ (Derwent *et al.*, 2007; Stroud *et al.*, 2008). During this photochemical process, oxidants of VOCs can transform nitric oxide (NO) into NO₂ without consuming significant O₃. Thus, O₃ can accumulate. In this studied geographic domain, the east side is adjacent to the Taiwan Central Mountain Range, where vegetation could be an important source of VOCs (Fig. 2), whereas the west side is the coastal areas where is congested with large population and emits anthropogenic pollutants.

The OH radical is a highly reactive species and that formation relies on the abundance of solar radiation (Paulson *et al.*, 1999; Alicke *et al.*, 2003). Notably, OH radical can react with numerous reduced gases such as VOCs and NO_x in the atmosphere (Stroud *et al.*, 2008). Atkinson *et al.* (1989, 1991, 1990 and 2000) measured the reaction rate constant of alkanes, alkenes and aromatic series with OH. The results showed that alkenes have higher reactivity and thus O₃ formation potential compared to alkanes and aromatics in photochemical reactions.

OH is constantly generated and consumed in polluted air and; thus, its high reactivity forbids its accumulation, rendering its concentration in the atmosphere at an extremely low level (about 1×10^6 molecule/cm³ on average). Despite of its low level, OH

* Corresponding author. Tel.: +886-4-22853411;
Fax: +886-4-22862587
E-mail address: tsuang@nchu.edu.tw

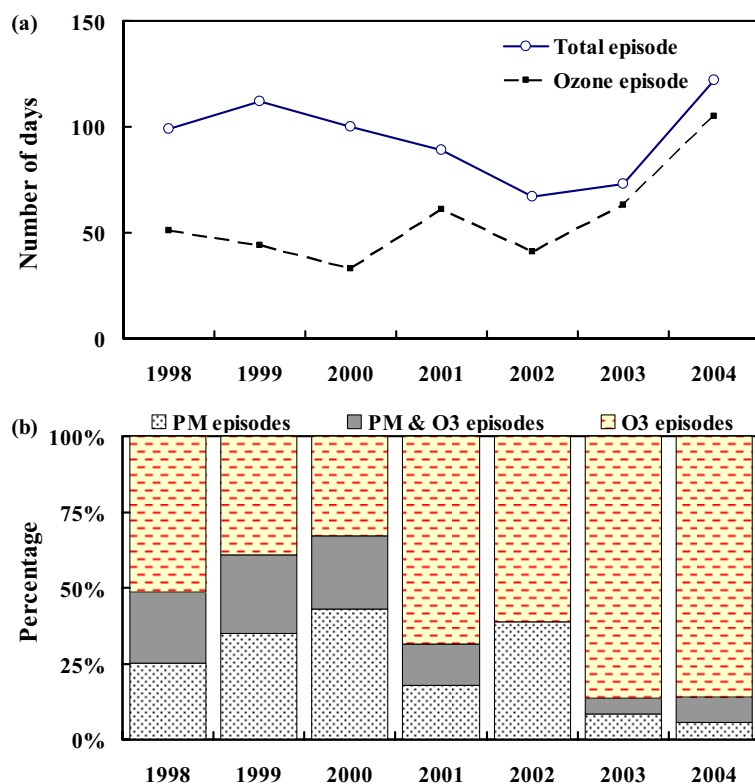


Fig. 1. The statistical results of air pollution episode days at Jhushan station from 1998 to 2004. (a) The total number of episode days (solid thin) and O₃ episode days (short dash). (b) The percentage of various air pollution episode days including PM episode days (black mesh), O₃ episode days (red mesh) and O₃ with PM episode days (gray bar).

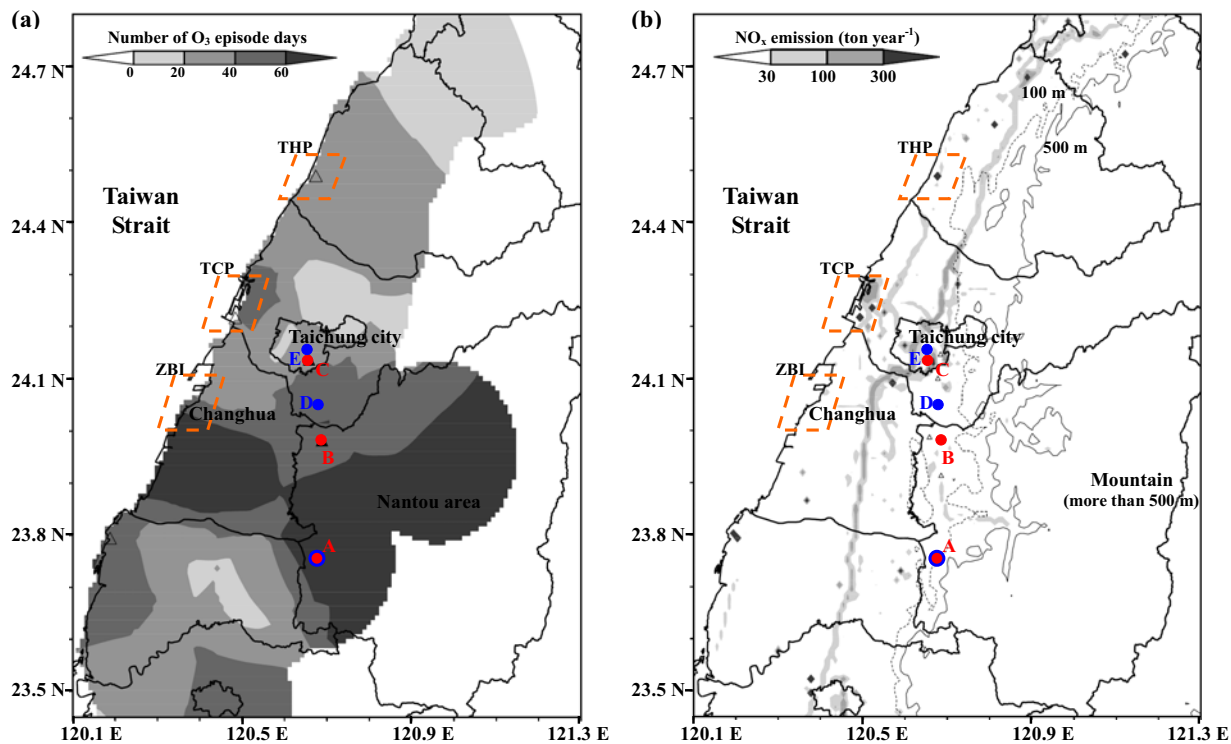


Fig. 2. Map of Central Taiwan shows the distribution of pollutant sources at Tungshiao power plant (THP), Taichung power plant (TCP) and Zhangbin industrial district (ZBI) as well as the distribution of study sites and monitoring stations, including Jhushan PAMS with AQMS (A); Caotun PAMS (B); Chonglun PAMS (C); Dali AQMS (D) and Chungming AQMS (E). (a) The shaded area represents the number of the O₃ episode days in 2003, where the dark region described the total O₃ episode days were more than 60 days in the year. (b) The shaded area represents the NO_x emission and the height contours of 100 m (short dash) and 500 m (solid thin) are also shown.

plays an important role in photochemical reactions in the atmosphere, especially in the reaction of the O₃ formation process (Fenske et al., 2000; Martinez et al., 2003; Ren et al., 2003; Ren et al., 2006).

Due to the highly reactive characteristic of OH, its spatial and temporal distributions are highly variable. Therefore measuring OH concentration directly is challenging (Kovacs et al., 2003; Ren et al., 2008); however, OH concentration in the atmosphere can be estimated indirectly through an empirical formula or kinetic equation (Perner et al., 1987; Kramp and Volz-Thomas, 1997; Derwent et al., 1999; Forberich et al., 1999). For instance, Cunnold et al. (1978) utilized CH₃CCl₃ long-term observation data and its emission data to indirectly calculate the average atmosphere OH concentration.

The main purpose of this study is to analyze the observation data of three PAMS in central Taiwan. Based on the reaction rate differences for VOCs with OH, this study established a group of air aging photochemical indices and linked them with the level of O₃ concentration. This study also compared of the relationship of O₃ concentration and photochemical index between the upwind and downwind sites. Furthermore, OH concentrations were estimated base on the photochemical indices.

METHODOLOGY

Site and Field Campaign Description

In this study, the study area is in central Taiwan (Nantou County) on the west side of the Central Mountain Range (The altitude are greater than 500 m, Fig. 2). This area has abundant vegetation as a potential natural source of VOCs emissions; the types of vegetation include farmlands, grasslands, broadleaf tree and coniferous forest. Except for the highly reactive species coming from industrial activity, traffic and transportation upwind (e.g., Taichung city and Changhua city, Fig. 2(b)), the plants along the transmission path is also a very important source of VOCs and NO_x. Moreover, for NO_x other than vehicular and industrial sources, large power plants (i.e., Taichung power plant (TCP) and Tunghsiao power plant (THP), Fig. 2(b)) are also important sources. As a result, high O₃ episodes at downwind of the stack plumes (such as Jhushan and Caotun) are to be expected (Fig. 2) (Ryerson et al., 2001).

Fig. 2 shows the distribution of the number of O₃ episode days in central Taiwan in 2003. There were more than sixty O₃ episode days in Nantou area in 2003 and Jhushan was regarded as a typical site for high-ozone concentrations although it located in rural site. The VOC data set from the three PAMS and three adjacent AQMS were analyzed for the evidence of photochemical process from upwind to downwind site (Fig. 2 and Table 1).

Surface VOC measurements were performed by the network of three PAMS at Chonglun PAMS (120°39'29.0" E, 24°07'59.2" N), Caotun PAMS (120°41'18.5" E, 23°58'44.9" N) and Jhushan PAMS (120°40'37.2" E, 23°45'23.4" N). The Chonglun PAMS was regarded as a typical upwind site, and the Jhushan PAMS was the downwind site. The Caotun PAMS was in the midway of the transport path acting as an authentication station. Thus, a complete line of observation comprising upwind-downwind transport was established. This network performs year-round hourly measurements of 55 VOCs from C₂-C₁₂ (Table 1). The analytical instruments of Taiwan PAMS are similar to those used in U.S. PAMS. Details of the analytical instrument can refer to earlier publications by Wang et al. (2005) and Yang et al. (2005). Moreover, the AQMS were located in the vicinity of each PAMS, including Jhongming AQMS (120°39'33.1" E, 24°09'29.8" N), Dali AQMS (120°40'40.0" E, 24°05'58.1" N) and Jhushan AQMS (120°40'37.2" E, 23°45'23.4" N). Jhongming AQMS is upward; Jhushan AQMS is downwind and Dali AQMS is the midway station, which also to form an upwind-to-downwind observation line.

Model System

The Gaussian Trajectory transfer-coefficient modeling system (GTx) was developed recently and has been certified by the Taiwan Environmental Protection Administration (Taiwan EPA) in 2007 (Tsuang, 2003; Tsuang et al., 2003a, b). The GTx, which consists of a main program (gtx.982) and its matching wind field trajectory model (Traj model, Traj.68), can be used to identify pollutant sources of a receptor (Hsieh et al., 2008). The trajectory model was developed in order to evaluate the routes of plumes from source by interpolating hourly meteorological data observed from Taiwan Central Weather Bureau (CWB/Taiwan), Taiwan EPA and Taiwan Power Company. In addition, the vertical profiles of wind fields and air temperature collected by the tethered system were also used for determining the trajectories (Chen et al., 2002). The horizontal wind vector at each trajectory grid is calculated by considering the distance and the height between the receptor and each station. The vertical wind vector is calculated according to the continuity equation of an incompressible flow (e.g. White, 1991). The stability at each trajectory grid is based on Pasquill stability (Seinfeld, 1986), and the mixing height is determined by the Holzworth method (Holzworth, 1972).

The receptor in this study was set at Jhushan station, and the period of backward trajectory was set as 72 hours. The height of the backward trajectory line started from 50 meters above ground level and changed with the terrain and the meteorological condition along the trajectory line.

Table 1. Details of the Chonglun, Caotun and Jhushan PAMS, as well as the name of 55 VOCs species from C₂-C₁₂.

PAMS	Location	Environment
Chonglun (Upwind)	120°39'29.0" E 24°07'59.2" N	This site locates in a typical City Park with many trees. The park surrounded with major access road and surrounded by buildings.
Caotun (Midway)	120°39'54.8" E 023°58'07.6" N	This site is mostly rice paddy without high emission industries; it is dozens of meters away from road and its traffic flow is low.
Jhushan (Downwind)	120°40'37.2" E 023°45'23.4" N	This site is surrounded with spacious field and without high pollution industry; its population, house and traffic density are low.
Monitoring of species		
Ethane, Ethylene, Propane, propylene, iso-Butane, Acetylene, n-Butane, t-2-butene, 1-Butene, cis-2-Butene, Cyclopentane, iso-Pentane, n-pentane, t-2-pentene, 1-pentene, c-2-pentene, 2,2-dimethylbutane, 2,3-dimethylbutane, 2-methylpentane, 3-methylpentane, iso-prene, n-Hexane, Methylcyclopentane, 2,4-Dimethylpentane, Benzene, Cyclohexane, 2-Methylhexane, 2,3-Dimethylpentane, 3-Methylhexane, 2,2,4-Trimethylpentane, n-Heptane, Methylcyclohexane, 2,3,4-Trimethylpentane, Toluene, 2-Methylheptane, 3-Methylheptane, n-Octane, Ethylbenzene, m,p-Xylene, Styrene, o-Xylene, n-Nonane, Isopropylbenzene, n-Propylbenzene, m-Ethyltoluene, p-Ethyltoluene, 1,3,5-Trimethylbenzene, o-Ethyltoluene, 1,2,4-Trimethylbenzene, n-Decane, 1,2,3-Trimethylbenzene, m-Diethylbenzene, p-Diethylbenzene, n-Undecane, n-Dodecane.		

Photochemical Index

Because reactivity of VOCs in terms of O₃ formation is compound dependent, the reaction rate constant (k_{OH}) at which each species reacting with OH is used as the potential O₃ production. According to the kinetic equation, the species concentration gradually reduced as time increased. The compounds with larger k_{OH} decrease faster than that with smaller k_{OH} given the same time period. It is a common practice to exploit ratios of VOCs of similar sources and with a significant difference in reactivity. The ratios as indices can be used to assess the degree of a photochemical process. High ratios indicate that air masses are depleted in regard to reactive compounds (denominators); this translates into photochemical aged air masses, whereby the amount of O₃ produced increases. Low ratios produce an opposite result.

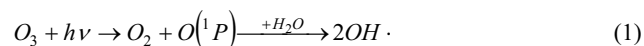
In this study, the VOCs species selected as photochemical index substance were measured and calculated the ratios of species concentration base on the difference in reaction rate. Using the photochemical index facilitates the verification of self-consistency and can be used to assess the correlation between O₃ concentration and the aging degree of an air mass. For example, ethylbenzene, m-xylene and p-xylene all mainly came from vehicle exhaust in a typical urban environment. Since m-xylene and p-xylene cannot be separated by chromatography, they were reported as a combined value (m, p-xylene). The reaction rates of ethylbenzene and m, p-xylene were 7.1 × 10⁻¹² cm³/molecule/s and 21.67 × 10⁻¹² cm³/molecule/s, respectively. In this study, the ratio of ethylbenzene to m, p-xylene was used as a photochemical index for air masses (Chang et al., 2006; Tsai et al., 2008; Wang et al., 2008).

The species concentrations were measured by PAMS in the upwind and the downwind. When an air mass is transported toward the downwind area, the species will be simultaneously subjected to the identical photochemical loss process, making the more reactive VOC decreasing faster than the less reactive one. By taking the ratio of a less reactive species to a more reactive species, the ratio tends to be constant in the source area dominated by fresh emissions, but could increase as an air parcel is subject to photochemical process during transport as the more reactive species decreases more rapidly.

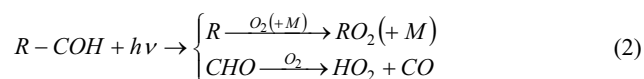
This study take ethylbenzene and m, p-xylene as example of a photochemical index that can calculate a ratio of ethylbenzene/m, p-xylene. Using the photochemical index, the aging degree of an air mass can be determined. The purpose of this study was to discuss the characteristic differences of the photochemical index and O₃ concentration between upwind and downwind, such as Chonglun, Caotun and Jhushan PAMS.

HO_x Reaction Mechanism

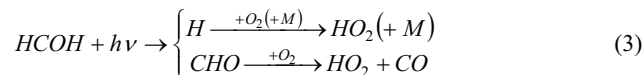
The HO_x radicals in the atmosphere include the OH radical and HO₂ radical. These HO_x radicals mainly produced by the photolysis of O₃ (Eq. (1)). The efficiency of photolysis depends on ultraviolet wavelength, O₃ and water vapor abundance, as well as sun intensity; as a result, it is highly susceptible to altitude, latitude and seasonality.



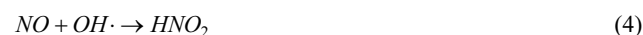
In addition, some organic compounds under certain circumstances would be a source of HO_x in the atmosphere. For example, when the O₃ concentration is not high, aldehydes (general formula: R-COH) could become an important source of OH radical (Eq. (2)).



where R-stands for alkyl group or H (Seinfeld and Pandis, 1998). Using the methanal (HCOH) as an example, its main sources are from the regional emissions or generated by the CO conversion. The reaction equation of methanal is shown in Eq. (3).



In addition, the photolysis of nitrite (HNO₂) is also an important source of OH radicals in the atmosphere. At the general atmospheric environment, the OH radicals react with nitric oxide (NO) to produce NHO₂ without photolysis reaction (Eq. (4)). However, in early morning, HNO₂ was recycled back to OH and NO rapidly through the Eq. (5) (Jenkin and Clemitshaw, 2000; Lin et al., 2006).



The OH concentration is extremely low and it varies considerably with time and space, which makes directly measuring OH concentrations extremely difficult. This study uses the observed data of PAMS at different locations, air masses trajectory and kinetic equations to estimate the concentrations of OH radical in the atmosphere.

RESULTS

The increased proportion of O₃ episode days has become a much more serious concern. In recent years, the number of total episode days are decreasing year by year at Jhushan PAMS, but the episode days caused by O₃ pollution are an increasing trend, with approximately 90 percent of O₃ episode days in 2003 (Fig. 1). This study focused on the data analysis and the simulation of air mass trajectory in 2003. Moreover, the photochemical index ratio of ethylbenzene/m, p-xylene was determined in order to identify the degree of photochemical reactions in this study.

Backward Trajectory and Residence Time

From the backward trajectory simulations, the routes of air masses transported to the receptor can be estimated, and then evaluate the location of potential source. Thus, three PAMS were set as the targets of backward trajectories in this study. In the prevailing northern wind season, Jhushan PAMS was set as a receptor (the downwind station) and Chonglun and Caotun PAMS were set as sources (the upwind stations). The backward trajectories starting from Jhushan PAMS and passing through both distances within 2.5 kilometers around Caotun or Chonglun PAMS were chosen to discuss the relationship between air mass's transmission time and pollutant concentrations.

According to the results of the backward trajectory simulation, the days when air masses passed through the three PAMS at the same trajectory totaled to 101 days in 2003; the dates were mainly distributed in the fall, winter and spring, which are the seasons of strong northeast monsoons (Fig. 3). We find that 30% of ozone episodes occurred in Jhushan PAMS is with the backward trajectories passed through Chonglun and Caotun PAMS. These phenomena infer that the O₃ concentrations in the downwind area were related to the air mass transmission from the upwind area, especially on the O₃ episode days.

Figs. 4(a) and 4(b) show the distribution map of the backward trajectories and the hourly maximum of O₃ concentration on May 26th and October 17th, respectively. The results clearly show that the trajectories were impacted by the northeast monsoon, and the hourly maximum O₃ concentrations near Jhushan PAMS were

higher than other areas in central Taiwan. The trajectories also indicated that the transporting of an air mass from Chonglun PAMS (upwind) to Jhushan PAMS (downwind) took 4 hours on May 26th and 8 hours on October 17th. By calculating all of the

trajectories in 98 days, the mean residence time was 4.8 hours for an air mass transported from Caotun PAMS to Jhushan PAMS, and 7.0 hours for from Chonglun PAMS to Jhushan PAMS.

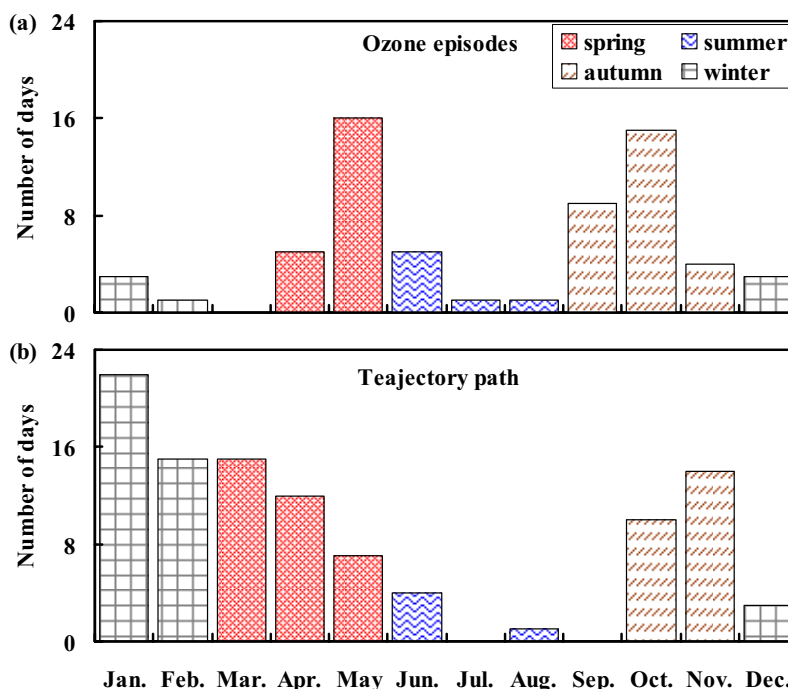


Fig. 3. (a) The number of O₃ episode days for each month in 2003. (b) The number of days for the air mass on the same trajectory path passed through Chonglun, Caotun and Jhushan PAMS.

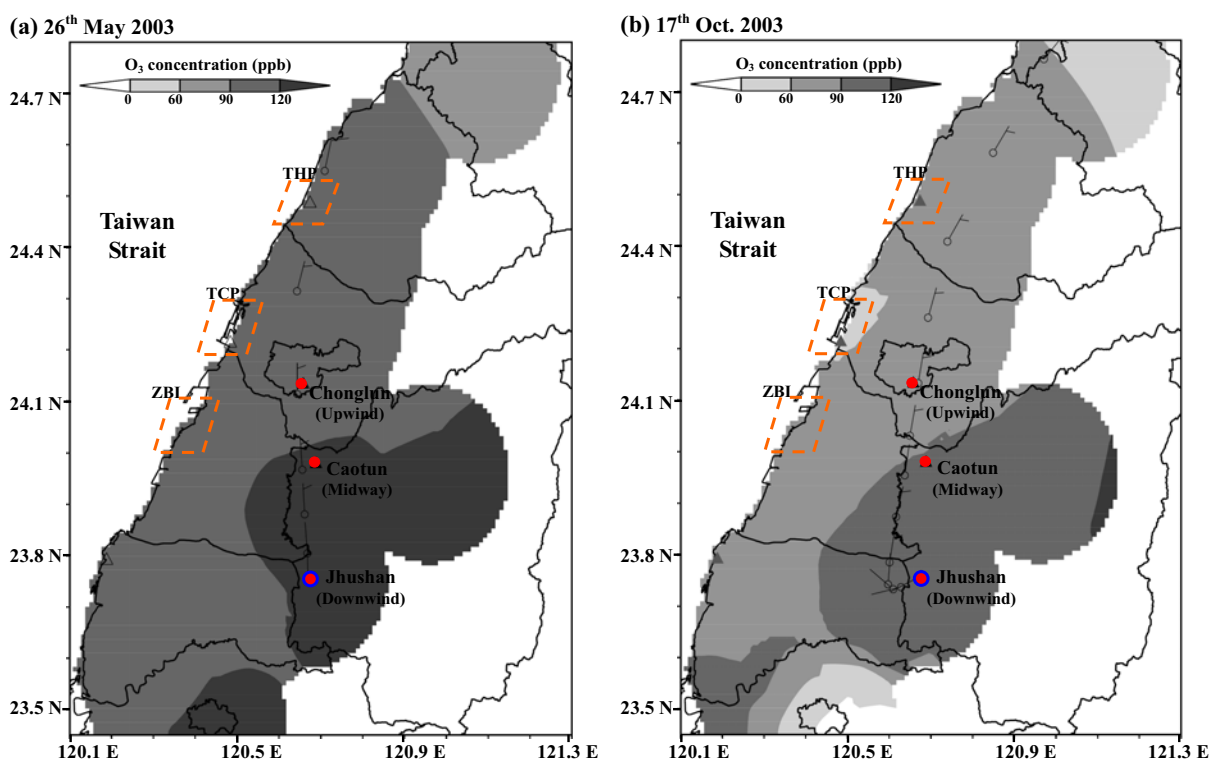


Fig. 4. The schematics of distribution for backward trajectories of an air mass passed through the three PAMS, where Jhushan PAMS was set as a receptor for the trajectory model. The shaded area represents the maximum hourly O₃ concentration also shown on (a) 26th May 2003 and (b) 17th October 2003.

Time Series and Diurnal Cycle of Compound Concentration

In this study, the two compounds (ethylbenzene and m, p-xylene) were used for a photochemical index and to assess the

correlation between O_3 concentrations and the degree of photochemical reactions. Fig. 5 shows the time series of ethylbenzene and m, p-xylene concentrations measured by the

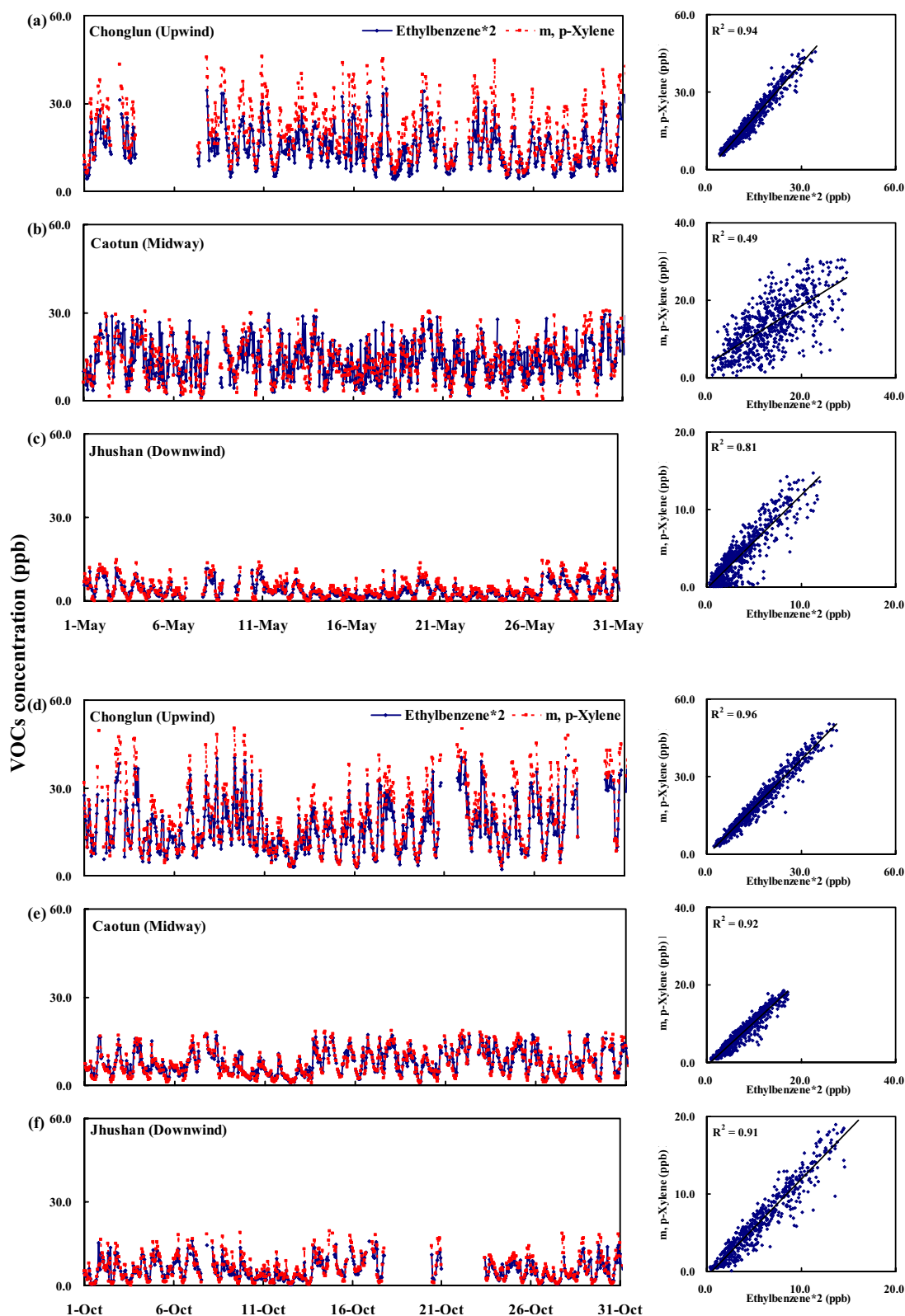


Fig. 5. The time series and X-Y plots of ethylbenzene and m, p-xylene hourly concentration measured by Chonglun, Caotun and Jhushan PAMS in May 2003 are shown on (a), (b) and (c), respectively and in October 2003 are shown on (d), (e) and (f), respectively. The R^2 showed the coefficients of determination for ethylbenzene and m, p-xylene hourly concentrations.

three PAMS throughout May and October 2003, since the number of O₃ episode days are higher in May and October.

As Fig. 5 illustrates, the concentrations of ethylbenzene and m, p-xylene in Chonglun PAMS were higher than those in Caotun and Jhushan PAMS, whether in May or October. The maximum concentration of ethylbenzene and m, p-xylene at three PAMS are, in descending order: Chonglun > Caotun > Jhushan. This phenomenon is due to the Chonglun PAMS being located upwind in the city where there are a lot of emission sources from the traffic. The determination of correlations (R^2) of ethylbenzene and m, p-xylene concentrations at Chonglun, Caotun and Jhushan PAMS were 0.94, 0.49 and 0.81 in May and 0.96, 0.92 and 0.91 in October, respectively. The results indicated the aged air parcels passed Chonglun, Caotun and Jhushan PAMS and had the same source emitted from the transportation vehicle exhaust.

The hourly surface concentrations of ethylbenzene and m, p-xylene were compared at three PAMS. Fig. 6 shows their composite hourly means concentration of ethylbenzene and m, p-xylene throughout May and October 2003. Higher concentrations of the two compounds were observed during the morning (06-08 LT, "LT" is the acronym of "local time") and evening (18-20 LT) rush hours (Fig. 6). The results indicate that the origin of these two compounds are mainly emitted from vehicles in the upwind site (Chonglun and Caotun PAMS) and become well mixed after transporting to the downwind site (Jhushan PAMS). Moreover, the concentrations of the two compounds during the daytime (09-17 LT) were lower than those during the nighttime (18-08 LT), due to the photochemical reactions and atmospheric turbulence being stronger in daytime.

Time Series and Diurnal Cycle of Photochemical Index

This study chose ethylbenzene/m, p-xylene as an air mass photochemical index. Fig. 7 shows the time series of daily mean

value of photochemical index (ethylbenzene/m, p-xylene) which calculated by the observation data at three different PAMS (Chonglun, Caotun and Jhushan PAMS) throughout 2003.

The values of average daily photochemical index ratios for three PAMS are, in descending order: Jhushan (0.51) > Caotun (0.49) > Chonglun (0.40). This phenomenon is due to the location of the three PAMS. Chonglun located at the upwind near the emission source and Jhushan PAMS was at the downwind of the transmission path. As the transmission time of the air mass in the atmosphere increases, the value of photochemical index also increases. Moreover, the values of daily photochemical index are higher in the spring (March-May). This phenomenon in the Jhushan PAMS is more pronounced and Caotun PAMS also has this trend. This season also easily leads to increased O₃ pollution.

Fig. 8 shows the composite hourly values of photochemical index (Chonglun, Caotun and Jhushan PAMS) and O₃ concentrations (Jhongming, Dali and Jhushan station) between the upwind and downwind throughout 2003. The photochemical index reaches maximum at noon to early afternoon on a daily cycle at the three PAMS. The maximum of the mean photochemical index at Chonglun, Caotun and Jhushan PAMS are 0.46, 0.70 and 1.02, respectively, which are, in descending order: Jhushan (downwind) > Caotun (midway) > Chonglun (upwind).

DISCUSSION

Correlation between Ozone Concentration and Photochemical Index

Ozone is a secondary pollutant and a major product of photochemical reactions of VOCs in the presence of NO_x. During the photochemical process, the concentration of VOC species decrease with the reaction time. In this study, the photochemical

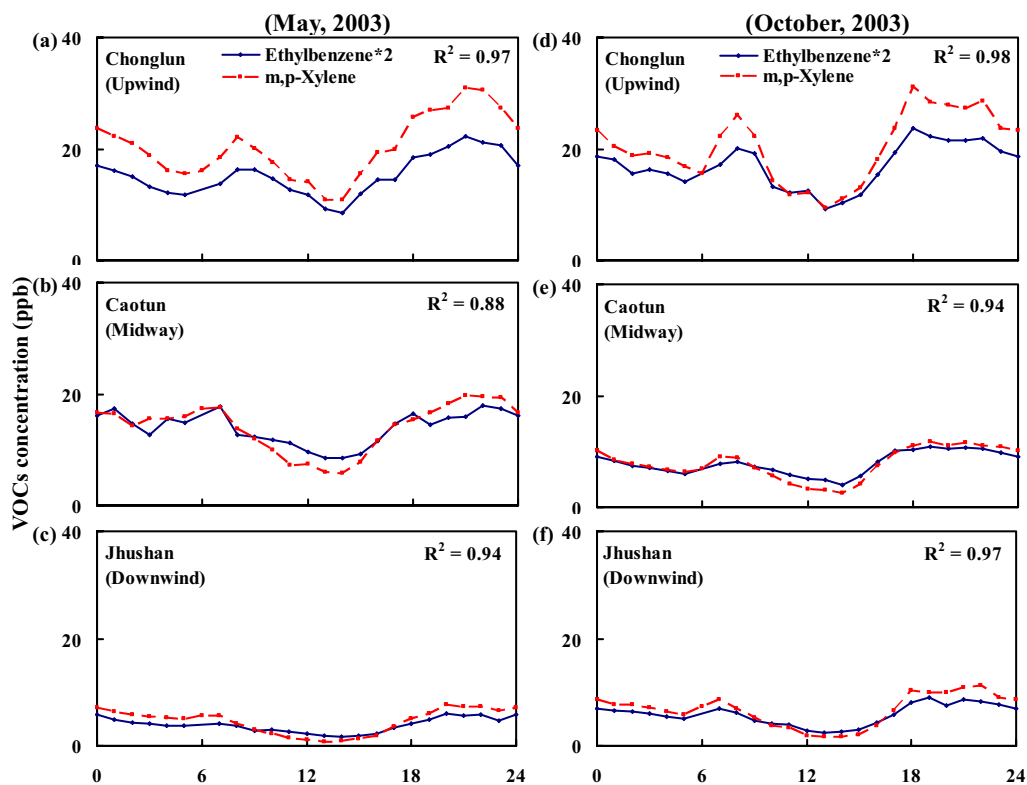


Fig. 6. Composite hourly concentrations of ethylbenzene and m, p-xylene at Chonglun, Caotun and Jhushan PAMS on May 2003 are shown on (a), (b) and (c), respectively and on October 2003 are shown on (d), (e) and (f), respectively. The R^2 showed the coefficients of determination for ethylbenzene and m, p-xylene composite concentrations.

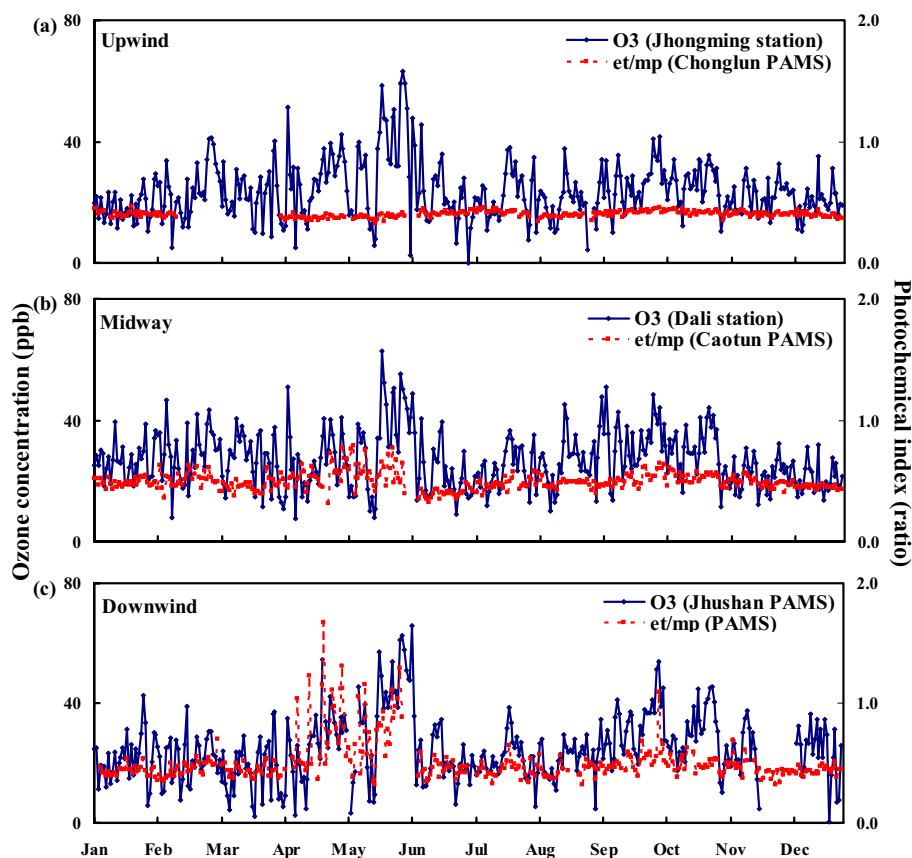


Fig. 7. The time series of daily ratio of ethylbenzene to m, p-xylene (et/mp) at Chonglun, Caotun and Jhushan PAMS throughout 2003, as well as the O₃ daily concentrations at the three corresponding air quality stations Chungming, Dali and Jhushan are also shown.

index (ethylbenzene/m, p-xylene) was determined to identify the degree of photochemical reactions, or the so-called “age” of an air mass, which should be moderately correlated with O₃ concentration within the same air mass (Chang *et al.*, 2006; Tsa *et al.*, 2008; Wang *et al.*, 2008). The value of ethylbenzene/m, p-xylene will increase along the path of transport. This phenomenon indicated that this air mass is aging, whereby the amount of O₃ produced increases. This comparison between the photochemical index and O₃ concentration shows that the correlation fluctuates strongly (Figs. 7 and 8).

The diurnal cycles of O₃ concentration were nearly synchronous with photochemical index ratio. The maximum of hourly average O₃ concentration occurs around noon to early afternoon at Jhongming, Dali and Jhushan stations that is similar to the photochemical index on daily cycle (Fig. 8). The results indicate that the photochemistry drives the diurnal cycles of the photochemical index ratios and O₃ concentration. The composite daily cycle of the photochemical index (ethylbenzene/m, p-xylene) and the O₃ concentration are strongly correlated with the determination of correlation (R²) of 0.65, 0.89 and 0.89 (Fig. 8) for the Chonglun, Caotun and Jhushan PAMS respectively. These phenomena demonstrate the cause-and-effect relationship between precursors and O₃ within the same air mass.

As an air mass is transported downwind from a source area, the photochemical index tends to increase. The photochemical index ratio at Jhushan PAMS is higher than those at Caotun and Chonglun PAMS (Figs. 7 and 8). The maximum O₃ concentrations at the three stations has the same trend which are, in descending order: Jhushan AQMS (69 ppb) > Dali AQMS (61 ppb) > Jhongming AQMS (60 ppb), where Jhongming AQMS is situated upwind and Jhushan AQMS downwind (Fig. 2 and 8).

This phenomenon indicates that the air mass in the downwind area is older than the air mass upwind. Furthermore, it is suitable for using VOC ratios as indicators of air mass age.

In comparing the photochemical index with the O₃ concentration, it shows that they have similar trends and good correlation. Therefore, when large photochemical indicator value happened, it may result in high O₃ pollution. The photochemical index can be indicative of the O₃ concentrations at noon and early afternoon and tie in with the trajectory model to estimate the concentration of other species, such as OH radicals.

Estimate the Concentration of OH Radicals

Based on the first order kinetic equation ($N = N_0 \exp(-kt[\text{OH}])$), the concentration of species gradually decreases with the reaction time increases. Two VOCs species of A and B are considered to pack into the kinetic equation, and the equation becomes as follows:

$$\begin{cases} [A]_{t=t} = [A]_{t=0} \cdot \exp(-k_A[\text{OH}] \times t) \\ [B]_{t=t} = [B]_{t=0} \cdot \exp(-k_B[\text{OH}] \times t) \end{cases} \quad (6)$$

where A and B are concentrations of two VOCs species of photochemical index; k_A and k_B are reaction rate constants of A species and B species, respectively; and t is the residence time for air masses emitted into the atmosphere that is proportional to the distance of air mass. When $t = 0$, which represents the air mass is at the location of emission sources or upwind. When $t = t$, which represents the time t for transmission. This signifies that an air mass is located in the receptor points or downwind.

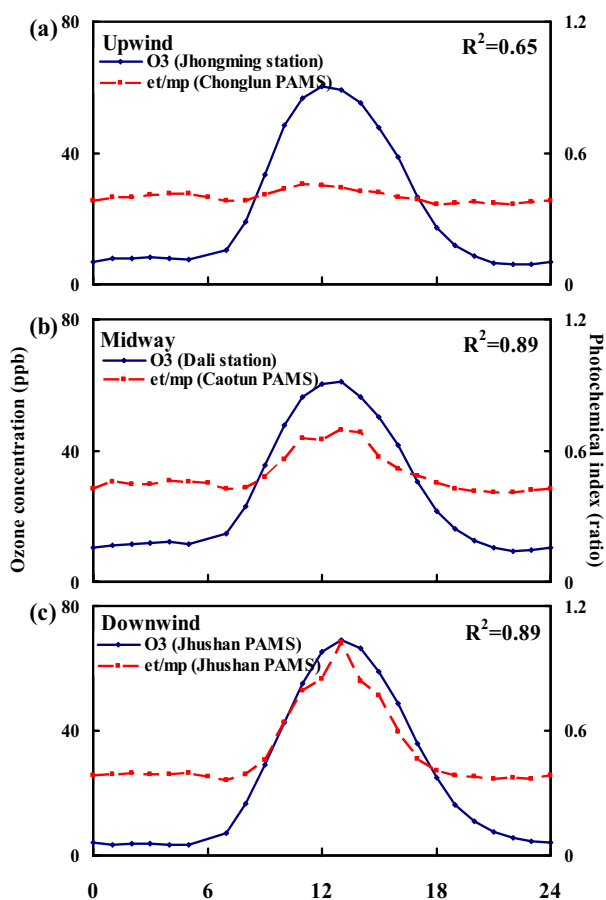


Fig. 8. Composite hourly ratio of ethylbenzene to m, p-xylene (et/mp) and O₃ concentration at the upwind, midway and downwind area throughout 2003. The R² showed the coefficients of determination of composite hourly ratio (et/mp) and O₃ concentration for each area.

After Eq. (6) is simplified and take its natural logarithm, Eq. (6) can be rewritten as Eq. (7) and (8):

$$M = N \cdot \exp(k_B - k_A)[OH] \times t \quad (7)$$

$$\ln(M/N) = (k_B - k_A)[OH] \times t \quad (8)$$

where $M = ([A]/[B])_{t=t}$ is the photochemical index after time t for transmission, which means the aged air mass. $N = ([A]/[B])_{t=0}$ signifies the photochemical index of the emissions source or fresh air mass. Therefore, $\ln(M/N)$ can be expressed as an indicator of aging degree of an air mass (Eq. (8)). When $\ln(M/N)$ increases, it is considered that the aging degree of an air mass also increases.

In terms of ethylbenzene and m, p-xylene for example, ethylbenzene and m, p-xylene represents the A and B of Eq. (6) respectively. Moreover, k_A is the reaction rate constant of ethylbenzene and k_B is the reaction rate constant of m, p-xylene. These two species concentrations were monitored at PAMS. These data could be incorporated into the Eq. (8), and estimated the $[OH] \times t$.

The value of $[OH] \times t$ is the calculation result of the species concentration and reaction rate constant, such as $(\ln(M/N))/(k_B - k_A) = [OH] \times t$. Therefore, when the residence time t of species in the atmosphere can be determined, the instantaneous concentration of OH can be estimated. In this study, the GTx model was used to carry out the simulation of backward trajectory and calculated residence time t of species in the atmosphere. The result of residence time (t) of air masses indicated that transporting an air mass from Caotun PAMS (upwind) to Jhushan PAMS (downwind) took 1-18 hours and is 2-24 hours for from Chonglun PAMS to Jhushan PAMS.

Both the OH concentrations calculated from Caotun PAMS to Jhushan PAMS and from Chonglun PAMS to Jhushan PAMS have similar trends on the daily cycle. The results indicate that the maximum of OH concentration reach to $2.1 \times 10^6 - 2.3 \times 10^6$ molecule/cm³ at noon to early afternoon and minimum at night in the region around Jhushan PAMS (Fig. 9). Table 2 shows the maximum OH concentrations in field measurement and model simulation in some researches. In this study the OH concentrations obtained by mean of calculating ethylbenzene/m, p-xylene in aged air parcel at Jhushan PAMS are in the same range as other studies. The result showed that the photochemical index method can provide a good OH estimation. The average hourly OH concentration calculated from Caotun PAMS to

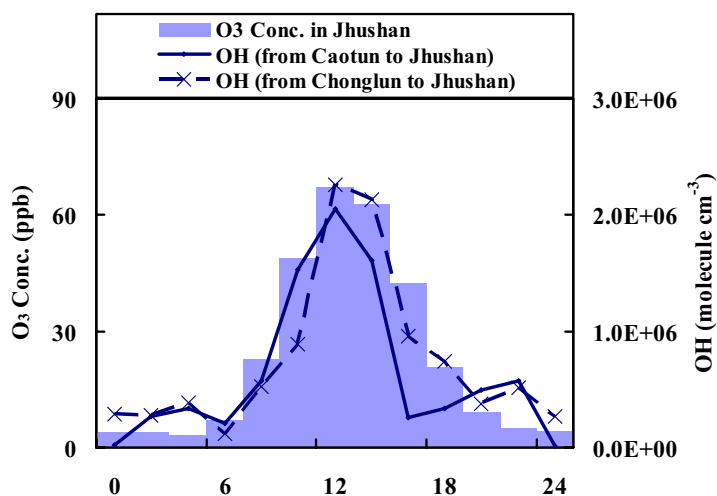


Fig. 9. The estimated results of the O₃ and OH concentration at 2-hour intervals in Jhushan PAMS. The shaded area represents the O₃ concentration. The blue lines represent the OH concentration which calculated from Caotun PAMS to Jhushan PAMS (short dash) and from Chonglun PAMS to Jhushan PAMS (solid thin).

Table 2. Maximum OH concentrations in field measurement and model simulation.

Reference	Maximum OH concentration (molecule/cm ³)	
Perner <i>et al.</i> (1987)	0.7 to 3.2	(observed)
Comes <i>et al.</i> (1997)	2.0 to 6.0	(observed)
George <i>et al.</i> (1999)	1.0	(observed)
Ren <i>et al.</i> (2003)	5.0 to 10.0	(observed)
Alicke <i>et al.</i> (2003)	2.0 to 8.0	(observed)
Ren <i>et al.</i> (2006)	1.3 to 2.6	(observed)
Ren <i>et al.</i> (2003)	5.0 to 10.0	(simulated)
Alicke <i>et al.</i> (2003)	4.0 to 16.0	(simulated)
Ren <i>et al.</i> (2006)	1.3 to 3.6	(simulated)
This study	2.1 to 2.3	(simulated)

Jhushan PAMS was 1.04×10^6 molecule/cm³ during the daytime (06-17 LT) and 3.39×10^5 molecule/cm³ during the nighttime (18-05 LT). Moreover, the OH concentration calculated from Chonglun PAMS to Jhushan PAMS was 1.15×10^7 molecule/cm³ and 4.27×10^5 molecule/cm³ during the daytime and nighttime respectively.

CONCLUSIONS

The monitoring network was used to measure O₃ and its precursor data from upwind to downwind in central Taiwan. In this study, the ethylbenzene and m, p-xylene were selected as suitable species for photochemical index based on the different reaction rate and consistent source. Moreover, the ratio of ethylbenzene to m, p-xylene can represent one kind of age indicators, and have high relevance with O₃ concentration.

The daily cycle of the photochemical index (ethylbenzene/m, p-xylene) and the O₃ concentration are strongly correlated with the determination of correlation (R²) greater than 0.65 for each PAMS. Both the maximum values of photochemical index and O₃ concentration appeared around noon and minimum values occurred at night. As an air mass is farther from the source area, the photochemical index ratio tends to increase for the photochemical processes. Classifying by station location, Chonglun PAMS is upward; Jhushan PAMS is downwind and Caotun PAMS is midway station. The photochemical index of three PAMS are descending order of Jhushan > Caotun > Chonglun. Descending order of O₃ concentration showed the same order of photochemical index in different areas (Jhushan > Dali > Jhongming). These results demonstrate that the photochemistry and reaction time drives the values of the photochemical index and O₃ concentration.

Moreover, the photochemical indexes of three PAMS with trajectory model, the residence time and kinetic equations were used to estimate the OH concentrations. The results show the OH concentrations are to reach the maximum (2.1×10^6 - 2.3×10^6 molecule/cm³) at noon to early afternoon on daily cycle in the region around Jhushan station. The daily cycle of OH concentration is similar to the daily cycle of O₃ concentration that due to OH plays an important role in the reaction of O₃ formation process.

ACKNOWLEDGMENTS

The authors are grateful for financial support from the National Science Council, Taiwan, under the contracts NSC-91-EPA-Z-005-004, NSC-92-2211-E-005-023, NSC-93-2211-E-005-006, NSC-94-2211-E-005-039, NSC 95-EPA-Z-005-001 and NSC 95-2111-M-005-001. Thanks to Dr. Arumugam Alagesan, Dr. Andrew Keats and Dr. Ted Knoy for

proof reading. We are also grateful to Pei-Hsuan Kuo, Chuen-Liang Horng, Ding-Cang Kuo, Mei-Chun Kuo, Jun-Nan Kuo, Co-Zi Yen and Yu-Chi Kuo for their assistance with the tethersonde operation.

REFERENCES

- Alicke, B., Geyer, A., Hofzumahaus, A., Holland, F., Konrad, S., Patz, H.W., Schafer, J., Stutz, J., Volz-Thomas, A. and Platt, U. (2003). OH Formation by HONO Photolysis during the BERLIOZ Experiment. *J. Geophys. Res.* 108: 8247. doi: 10.1029/2001JD000579.
- Atkinson, R. (1989). Kinetics and Mechanisms of the Gas-Phase Reactions of the Hydroxyl Radical with Organic Compounds. *J. Phys. Chem. Ref. Data*. Monograph. 1: 1-246.
- Atkinson, R. (1990). Gas-Phase Tropospheric Chemistry Organic Compounds: A Review. *Atmos. Environ. Part A*. 24: 1-41.
- Atkinson, R. (1991). Kinetics and Mechanisms of the Gas-Phase Reactions of the NO₃ Radical with Organic Compounds. *J. Phys. Chem. Ref. Data*. 20: 459-507.
- Atkinson, R. (2000). Atmospheric Chemistry of VOCs and NO_x. *Atmos. Environ.* 34: 2063-2101.
- Beckett, W.S. (1991). Ozone, Air Pollution, and Respiratory Health. *Yale J. Biol. Med.* 64: 167-175.
- Carter, W.P.L. (1994). Development of Ozone Reactivity Scales for Volatile Organic Compounds. *J. Air Waste Manage. Assoc.* 44: 881-899.
- Chen, C.L., Tsuang, B.J., Tu, C.Y., Cheng, W.L. and Lin, M.D. (2002). Wintertime Vertical Profiles of Air Pollutants over a Suburban Area in Central Taiwan. *Atmos. Environ.* 36: 2049-2059.
- Chang, C.C., Wang, J.L., Liu, S.C. and Candice Lung S.C. (2006). Assessment of Vehicular and Non-Vehicular Contributions to Hydrocarbons Using Exclusive Vehicular Indicators. *Atmos. Environ.* 40: 6349-6361.
- Comes, F.J., Forberich, O. and Walter, J. (1997). OH Field Measurements: A Critical Input into Model Calculations on Atmospheric Chemistry. *J. Atmos. Sci.* 54: 1886-1894.
- Cunnold, D., Alyea, F. and Prinn R. (1978). A Methodology for Determining the Atmospheric Lifetime of Fluorocarbons. *J. Geophys. Res.* 83: 5493-5500.
- De Leeuw, F.A.A.M. (2000). Trends in Ground Level Ozone Concentrations in the European Union. *Environ. Sci. Policy*. 3: 189-199.
- De Leeuw, F.A.A.M. (2002). A Set of Emission Indicators for Long-Range Transboundary Air Pollution. *Environ. Sci. Policy*. 5: 135-145.
- Derwent, R.G., Carslaw, N., Simmonds, P.G., Bassford, M., O'Doherty, S., Ryall, D.B., Pilling, M.J., Lewis, A.C. and Mcquaid, J.B. (1999). Hydroxyl Radical Concentrations Estimated from Measurements of Trichloroethylene during the EASE/ACSOE Campaign at Mace Head, Ireland during July 1996. *J. Atmos. Chem.* 34: 185-205.
- Derwent, R.G., Jenkin, M.E., Passant, N.R. and Pilling, M.J. (2007). Photochemical Ozone Creation Potentials (POCPs) for Different Emission Sources of Organic Compounds Under European Conditions Estimated with a Master Chemical Mechanism. *Atmos. Environ.* 41: 2570-2579.
- Fenske, J.D., Kuwata, K.T., Houk, K.N. and Paulson, S.E. (2000). OH Radical Yields from the Ozone Reaction with Cycloalkenes. *J. Phys. Chem. A*. 104: 7246-7254.
- Forberich, O., Pfeiffer, T., Spiekermann, M., Walter, J., Comes, F.J., Grigonis, R., Clemitshaw, K.C. and Burgess, R.A. (1999). Measurement of the Diurnal variation of the OH Radical Concentration and Analysis of the Data by Modelling. *J. Atmos. Chem.* 33: 155-181.
- Fuhrer, J., Skärby, L. and Ashmore, M.R. (1997). Critical levels for Ozone Effects on Vegetation in Europe. *Environ. Pollut.* 97:

- 91-106.
- George, L.A., Hard, T.M. and O'Brien, R.J. (1999). Measurement of Free Radicals OH and HO₂ in Los Angeles Smog. *J. Geophys. Res.* 104: 11643-11655.
- Holzworth, G.C. (1972). *Mixing Heights, Wind Speeds, and Potential for Urban Air Pollution throughout the Contiguous United States*. AP-101, U.S. EPA, Raleigh, NC.
- Hsieh, L.Y., Chen, C.L., Wan, M.W., Tsai, C.H. and Tsai, Y.I. (2008). Speciation and Temporal Characterization of Dicarboxylic Acids in PM_{2.5} during a PM Episode and a Period of Non-Episodic Pollution. *Atmos. Environ.* 42: 6836-6850.
- Hsieh, L.Y., Kuo, S.C., Chen, C.L. and Tsai, Y.I. (2009). Size Distributions of Nano/Micron Dicarboxylic Acids and Inorganic Ions in Suburban PM Episode and Non-Episodic Aerosol. *Atmos. Environ.* 43: 4396-4406.
- Jenkin, M.E. and Clemitshaw, K.C. (2000). Ozone and other Secondary Photochemical Pollutants: Chemical Processes Governing Their Formation in the Planetary Boundary Layer. *Atmos. Environ.* 34: 2499-2527.
- Judith, P., Pawson, S., Ryan, L., Fogt, J., Nielsen, E. and Neff, W.D. (2008). Impact of Stratospheric Ozone Hole Recovery on Antarctic Climate. *Geophys Res Lett.* 35: L08714. doi: 10.1029/2008GL033317.
- Kassomenos, P., Skouloudis, A.N., Lykoudis, S. and Flocas, H.A. (1999). Air-Quality Indicators for Uniform Indexing of Atmospheric Pollution over Large Metropolitan Areas. *Atmos. Environ.* 33: 1861-1879.
- Kovacs, T.A., Brune, W.H., Harder, H., Martinez, M., Simpasa, J.B., Frost, G.J., Williams, E., Jobson, T., Stroud, C., Young, V., Fried, A. and Wert, B. (2003). Direct Measurements of Urban OH Reactivity during Nashville SOS in Summer 1999. *J. Environ. Monit.* 5: 68-74.
- Kramp, F. and Volz-Thomas, A. (1997). On the Budget of OH Radicals and Ozone in an Urban Plume from the Decay of C₅-C₈ Hydrocarbons and NO_x. *J. Atmos. Chem.* 28: 263-282.
- Kumar, U., Prakash, A. and Jain, V.K. (2008). A Photochemical Modeling Approach to Uninvestigate O₃ Sensitivity to NO_x and VOCs in the Urban Atmosphere of Delhi. *Aerosol Air Qual. Res.* 8: 147-159.
- Last, J.M. (1993). Global Change: Ozone Depletion, Greenhouse Warming, and Public Health. *Annu. Rev. Publ. Health.* 14: 115-136.
- Leeuw, F.D., Sluyter, R., Breugel, P.V. and Bogman, F. (2000). Air Pollution by Ozone in Europe in 1999 and Summer 2000. European Environment Agency. European Topic Centre on Air Quality.
- Lin, Y.C., Cheng, M.T., Ting, W.Y. and Yeh, C.R. (2006). Characteristics of Gaseous HONO, HNO₃, NH₃ and Particulate Ammonium Nitrate in an Urban City of Central Taiwan. *Atmos. Environ.* 40: 4725-4733.
- Martinez, M., Harder, H., Kovacs, T.A., Simpasa, J.B., Bassis, J., Leshner, R., Brune, W.H., Frost, G.J., Williams, E.J., Stroud, C.A., Jobson, B.T., Roberts, J.M., Hall, S.R., Shetter, R.E., Wert, B., Fried, A., Alicke, B., Stutz, J., Young, V.L., White, A.B. and Zamora, R.J. (2003). OH and HO₂ Concentrations, Sources, and Loss Rates during the Southern Oxidants Study in Nashville, Tennessee, Summer 1999. *J. Geophys. Res.* 108: 4617. doi: 10.1029/2003JD003551.
- Martins, L.D. and Andrade, M.D.F. (2008). Ozone Formation Potentials of Volatile Organic Compounds and Ozone Sensitivity to Their Emission in the Megacity of São Paulo, Brazil. *Water Air Soil Pollut.* 195: 201-213.
- Paulson, S.E., Chung, M.Y. and Hasson, A.S. (1999). OH Radical Formation from the Gas-Phase Reaction of Ozone with Terminal Alkenes and the Relationship between Structure and Mechanism. *J. Phys. Chem. A.* 103: 8125-8138.
- Perner, D., Platt, U., Trainer, M., Hobbler, G., Drummond, J., Junkermann, W., Rudolph, J., Schubert, B., Volz, A. and Ehhalt, D.H. (1987). Measurements of Tropospheric OH Concentrations: A Comparison of Field Data with Model Predictions. *J. Atmos. Chem.* 5: 185-216.
- Ren, X., Harder, H., Martinez, M., Leshner, R.L., Oligier, A., Simpasa, J.B., Brune, W.H., Schwab, J.J., Demerjian, K.L., He, Y., Zhou, X. and Gao, H. (2003). OH and HO₂ Chemistry in the Urban Atmosphere of New York City. *Atmos. Environ.* 37: 3639-3651.
- Ren, X., Brune, W.H., Mao, J., Mitchell, M.J., Leshner, R.L., Simpasa, J.B., Metcalf, A.R., Schwab, J.J., Cai, C., Li, Y., Demerjian, K.L., Felton, H.D., Boynton, G., Adams, A., Perry, J., He, Y., Zhou, X. and Hou, J. (2006). Behavior of OH and HO₂ in the Winter Atmosphere in New York City. *Atmos. Environ.* 40: S252-S263.
- Ren, X., Olson, J.R., Crawford, J.H., Brune, W.H., Mao, J., Long, R.B., Chen, Z., Chen, G., Avery, M.A., Sachse, G.W., Barrick, J.D., Diskin, G.S., Huey, L.G., Fried, A., Cohen, R.C., Heikes, B., Wennberg, P.O., Singh, H.B., Blake, D.R. and Shetter, R.E. (2008). HO_x Chemistry during INTEX-A 2004: Observation, Model Calculation, and Comparison with Previous Studies. *J. Geophys. Res.* 113: D05310. doi: 10.1029/2007JD009166.
- Ryerson, T.B., Trainer, M., Holloway, J.S., Parrish, D.D., Huey, L.G., Sueper, D.T., Frost, G.J., Donnelly, S.G., Schauffler, S., Atlas, E.L., Kuster, W.C., Goldan, P.D., Hubler, G., Meagher, J. F. and Fehsenfeld, F.C. (2001). Observations of Ozone Formation in Power Plant Plumes and Implications for Ozone Control Strategies. *Science.* 292: 719-723.
- Seinfeld, J.H. (1986). *Atmospheric Chemistry and Physics of Air Pollution*, Wiley, New York.
- Seinfeld, J.H. and Pandis, S.N. (1998). *Atmospheric Chemistry and Physics from Air Pollution to Climate Change*, John Wiley & Sons, Inc., New York.
- Son, S.W., Polvani, L.M., Waugh, D.W., Akiyoshi, H., Garcia, R., Kinnison, D., Pawson, S., Rozanov, E., Shepherd, T.G. and Shibata, K., (2008). The Impact of Stratospheric Ozone Recovery on the Southern Hemisphere Westerly Jet. *Science.* 320: 1486-1489.
- Stroud, C.A., Morneau, G., Makar, P.A., Moran, M.D., Gong, W., Pabla, B., Zhang, J., Bouchet, V.S., Fox, D., Venkatesh, S., Wang, D. and Dann, T. (2008). OH-Reactivity of Volatile Organic Compounds at Urban and Rural sites Across Canada: Evaluation of Air Quality Model Predictions Using Speciated VOC Measurements. *Atmos. Environ.* 42: 7746-7756.
- Tsai, D.H., Wang, J.L., Wang, C.H. and Chan, C.C. (2008). A Study of Ground-Level Ozone Pollution, Ozone Precursors and Subtropical Meteorological Conditions in Ventral Taiwan. *J. Environ. Monit.* 10: 109-118.
- Tsuang, B.J. (2003). Quantification on the Source/Receptor Relationship of Primary Pollutants and Secondary Aerosols by a Gaussian Plume Trajectory Model: Part I—Theory. *Atmos. Environ.* 37: 3981-3991.
- Tsuang, B.J., Chen, C.L., Lin, C.H., Cheng, M.T., Tsai, Y.I., Chio, C.P., Pan, R.C. and Kuo, P.H. (2003a). Quantification on the Source/Receptor Relationship of Primary Pollutants and Secondary Aerosols by a Gaussian Plume Trajectory Model: Part II. Case Study. *Atmos. Environ.* 37: 3993-4006.
- Tsuang, B.J., Lee, C.T., Cheng, M.T., Lin, N.H., Lin, Y.C., Chen, C.L., Peng, C.M. and Kuo, P.H., (2003b). Quantification on the Source/Receptor Relationship of Primary Pollutants and Secondary Aerosols by a Gaussian Plume Trajectory Model: Part III—Asian Dust-Storm Periods. *Atmos. Environ.* 37: 4007-4017.
- Wang, J.H., Chang, C.C. and Wang, J.L. (2005). Peak Tailoring Concept in GC Analysis of Volatile Organic Pollutants in the Atmosphere. *J. Chromatogr. A.* 1087: 150.
- Wang, J.L., Wang, C.H., Lai, C.H., Chang, C.C., Liu, Y., Zhang, Y., Liu, S. and Shao, M. (2008). Characterization of Ozone Precursors in the Pearl River Delta by Time Series Observation

- of Non-Methane Hydrocarbons. *Atmos. Environ.* 42: 6233-6246.
- White, F.M. (1991). *Viscous Fluid Flow*. McGraw-Hill, New York, p. 611.
- Wilson, S.R., Solomon, K.R. and Tang, X. (2007). Changes in Tropospheric Composition and Air Quality Due to Stratospheric Ozone Depletion and Climate Change. *Photochem. Photobiol. Sci.* 6: 301-310.
- Yang, K.L., Ting, C.C., Wang, J.L., Oliver, W.W. and Chan, C.C. (2005). Diurnal and Seasonal Cycles of Ozone Precursors Observed from Continuous Measurements at an Urban Site in Taiwan. *Atmos. Environ.* 39: 3221-3230.
- Yang, H.H., Chen, H.W., Chi, T.W. and Chuang, P.Y. (2008). Analysis of Atmospheric Ozone Concentration Trends as Measured by Eighth Highest Values. *Aerosol Air Qual. Res.* 8: 308-318.

Received for review, May 1, 2009

Accepted, June 24, 2009